Journal of Hydrology 613 (2022) 128409

Contents lists available at ScienceDirect

Journal of Hydrology

journal homepage: www.elsevier.com/locate/jhydrol

Research papers

Identifying multivariate controls of water and nitrate in deep loess deposits under different land use types

Wangjia Ji, Yanan Huang, Bingbing Li, Zhi Li *

State Key Laboratory of Soil Erosion and Dryland Farming on the Loess Plateau, College of Natural Resources and Environment, Northwest A&F University, Yangling, Shaanxi 712100, China

ARTICLE INFO

This manuscript was handled by Huaming Guo, Editor-in-Chief, with the assistance of Tamotsu Kozaki, Associate Editor

Keywords:
Ratio of standardized water to standardized nitrate
Climate reconstruction
Soil physiochemical properties
Wavelet analysis
Loess Plateau
Land use conversion

ABSTRACT

Identifying the environmental factors controlling deep soil water and nitrate is important for the sustainability of vegetation and ecosystems. However, the combined effects of multiple factors at varying scales have been poorly understood, especially in those regions with thick vadose zones and deep-rooted plants. The aim of this study is to identify the multivariate controls of water and nitrate in seven > 13 m deep boreholes under different land use types on China's Loess Plateau. After measuring soil water and nitrate contents, the combined effects of climatic factors (precipitation, temperature, and potential evapotranspiration) and soil properties (soil texture, magnetic susceptibility, pH, EC, and soil organic carbon) were explored by wavelet analysis. Land use is the key factor regulating deep soil water and nitrate reservoirs, with high water deficit and low nitrate accumulation within 0–10 m under non-fertilized forestlands and shrublands. The positive and negative standardized ratios respectively suggested the synergistic and antagonistic relationships of water and nitrate under shallow- and deep-rooted vegetation. As the important agent for nitrate leaching, soil water is influenced by magnetic susceptibility and sand. Furthermore, soil water, pH, EC, and soil organic carbon are individually or simultaneously responsible for nitrate transport and transformation, especially at large scales (> 7.5 m). This study provides novel insights for vegetation and environmental management, and benefits the parameterizing of process-based hydrological and biogeochemical models at regional or global scales, especially in the deep unsaturated zones.

1. Introduction

Soil water is a key component of the Soil-Plant-Atmosphere Continuum (SPAC), and plays an important role in plant growth and groundwater recharge (Allison and Hughes, 1983; Gee and Hillel, 2006). The plantation of deep-rooted plants triggers soil water depletion because of canopy interception, root uptake, and evapotranspiration (Huang et al., 2021; Ji et al., 2021). Further, the surplus nitrogen (N) fertilizer in soils, which moves downward with soil water, potentially threatens ecosystem and human health due to the lower nitrogen use efficiency (NUE) of approximately 30–40 % (Ju et al., 2009; Sebilo et al., 2013; Vitousek et al., 1997). The accumulation effects under orchards and legacy effects under non-fertilized forestlands have been largely reported (Gao et al., 2021; Ji et al., 2020; Turkeltaub et al., 2018). The land use conversion from shallow- to deep-rooted vegetation significantly influences soil water and nitrate variability, and further has significant impacts on groundwater recharge and water quality (Huang et al., 2018; Huang et al., 2021). In addition to vegetation, the variations of soil water and nitrate are closely controlled by climate, topography, soil type, and their interactions (Dekker et al., 2007; Jackson et al., 2004). As such, it is essential to reveal the variations and controlling factors of water and nitrate for the sustainability of vegetation and ecosystems.

The predominant environmental factors of soil water and nitrate reservoirs vary with different scales and depths (Jiao et al., 2021; Padilla et al., 2018; Wang et al., 2020). Specifically, soil texture greatly contributes to soil water infiltration at the field and catchment scales, while climatic factors, atmospheric circulation, and geographical location dominate soil water movement at the regional and global scales (Gu et al., 2021; Li et al., 2021). For instance, it takes longer for soil water to move downwards in soils with higher clay and silt contents. Moreover, nitrate inputs are largely controlled by anthropogenic activities, such as fertilization regimes and tillage system (Fan et al., 2010; Gao et al., 2019). Soil water plays an indispensable role in transport processes of nutrient and/or pollutant. Additionally, soil N cycle is mostly driven by microorganisms, whose survival and growth greatly depend on soil

* Corresponding author.
E-mail address: lizhibox@nwafu.edu.cn (Z. Li).

https://doi.org/10.1016/j.jhydrol.2022.128409
Received 20 January 2022; Received in revised form 8 June 2022; Accepted 23 August 2022
Available online 28 August 2022

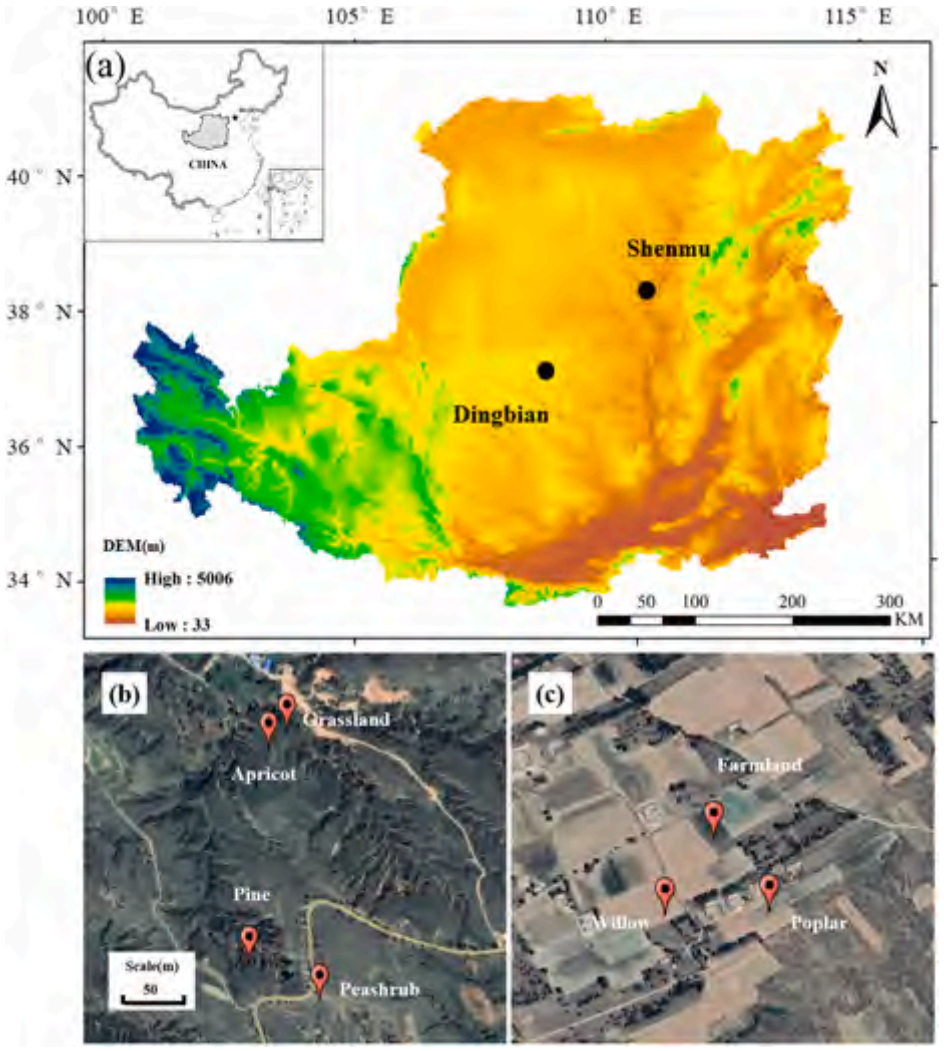

Fig. 1. Location of the study region on China's Loess Plateau (a), and distribution of the sampling sites in SM (b) and DB (c).

nutrient stoichiometry, regulated by aboveground litters, fine roots, root exudates and sloughs (Li et al., 2019a). These effects of environmental factors have been intensively investigated in topsoil and/or root zone (Niether et al., 2017; Yang et al., 2020; Zhao et al., 2011; Zheng et al., 2020), but their multivariate controls at different scales and depths are still unknown, especially in the regions with thick vadose zones and deep-rooted plants (Han et al., 2019; Jackson et al., 2004; Yu et al., 2019).

Traditional statistical analysis, e.g., (partial) correlation, linear regression, and principal component analysis, are mostly used to reveal the correlation between independent variables and different environmental factors at sampling scale (Lu et al., 2019; Zhu et al., 2018). Nevertheless, the hydrological and biogeochemical processes in the deep unsaturated zones are complicated and scale-dependent (Wiens, 1989), and multiple variables may individually or simultaneously contribute to a certain process. As an alternative, several advanced methods, e.g., empirical mode decomposition, multiple spectral coherence, and multiple wavelet coherence, have been proposed (Si, 2008). Specifically, wavelet analysis employs mathematical functions to explore the (non–) stationary processes occurring in limited time and space at multiple scales (Hu et al., 2017; Mihanović et al., 2009). The best factor and multi-factor combination at specific scale and location are further untangled (Si and Farrell, 2004). Considering the interactions of multiple environmental factors, the dominant factors of soil water and nitrate variability should be carefully considered by multiple methods at different depths and scales (Hu et al., 2017; Lu et al., 2019).

China's Loess Plateau, the largest loess covered area in the world (640,000 km^2, 100 million population), is ecologically fragile with very serious water loss and soil erosion (Fu et al., 2017; Jia et al., 2017b). Most cultivated farmlands have been converted into grasslands, shrublands, and forestlands since the 1950s (Li et al., 2017; Peng and Li, 2018), with vegetation cover improved by 28 % by 2013 (Chen et al., 2015). In the context of substantial land use conversion and deep vadose zones, the Loess Plateau is an ideal platform for exploring deep water and nitrate reservoirs, and their major environmental factors. In specific, high water deficit (~1000 mm) and nitrate-nitrogen (NO_3^--N) accumulation (~7250 kg N ha^{-1}) have been largely reported under deep-rooted fruit trees (Huang et al., 2021; Jia et al., 2018; Liu et al., 2019). Precipitation and potential evapotranspiration (ET_0) have greater contributions to soil water variability (Ye et al., 2019), while pH and soil texture may dominate nitrate variability (Yang et al., 2020). Identifying the variations and multivariate controls of water and nitrate improve their predictability, and further provide valuable information for hydrological and biogeochemical cycles in the thick loess deposits.

The objectives of this study are to identify the multivariate controls of water and nitrate in thick loess deposits under different land use types. Specifically, we try to answer the following questions: (i) How do soil water and nitrate contents relate to land use? (ii) How do multiple environmental factors combine to control soil water and nitrate? (iii) What are the implications for vegetation and environmental

Table 1
Detailed information of different sampling sites.

Location	P (mm)/ T (°C)/ ET_0 (mm)	Land use	Sampling depth (m)	Vegetation age (yr)	Location
SM	437/ 9.0/ 1104	Grassland	18	15	N38°47′51.17″ E110°22′18.68″
		Apricot	13.8	25	N38°47′50.03″ E110°22′17.34″
		Pine	15	25	N38°47′36.27″ E110°21′15.84″
		Peashrub	14.2	35	N38°47′33.79″ E110°21′21.20″
DB	332/ 8.6/ 1071	Farmland	18	–	N37°26′17.11″ E108°09′55.13″
		Willow	18	45	N37°26′12.34″ E108°09′51.78″
		Poplar	15	50	N37°26′12.58″ E108°09′58.95″

P, precipitation; T, temperature; ET_0, potential evapotranspiration.

management? This study provides essential information to the parameterizing of process-based hydrological and biogeochemical models at regional or global scales, especially in the thick unsaturated zones.

2. Materials and methods

2.1. Study area

Shenmu (SM) and Dingbian (DB) Counties were selected within the study region (Fig. 1a). With a continental monsoon climate (Jia et al., 2017a), the long-term (1957–2017) mean annual precipitation, temperature, and ET_0 in each location were shown in Table 1. Approximately 75 % of the rainfall occurred in the rainy season (June to September). In the two areas, the groundwater levels were 49 and 130 m below the ground. Sandy loam was the main soil texture with sand contents > 45 % (Zhu and Shao, 2008). Soil bulk density (SBD), field capacity (FC), and wilting humidity (WH) were 1.26 g cm^{-3}, 13 %, and 3 %, respectively. Three layers of loess, including Wucheng Loess (Q1, lower Pleistocene, 5–35 m), Lishi Loess (Q2, middle Pleistocene, 40–220 m), and Malan Loess (Q3, upper Pleistocene, 30–100 m), covered the mudstone and sandstone bedrock, with the paleosol layers distributed about 10 m below the surface. The cultivated farmland, mostly under wheat (*Triticum aestivum*) and maize (*Zea mays*) rotations, has been converted to non-fertilized grassland and shrub/forestland since the 1980s, including apricot (*Prunus* sp.), pine (*Pinus* sp.), peashrub (*Caragana arborescens*, a N-fixing food crop), willow (*Salix* sp.), and poplar (*Populus* sp.).

2.2. Sampling and analysis

Seven cores, deeper than 13 m under different land use types, were selected to be drilled in August 2017 (Table 1). They shared the similar climate, soil, and hydrological conditions, and thus reflected the land use change effects, to the greatest extent (Ji et al., 2020) (Fig. 1b&c). Synthetic fertilizer (Haber Bosch) and urea (about 132 kg N ha^{-1} yr^{-1}) were mostly used in cultivated farmland (wheat and maize), whereas other non-fertilized lands were respectively transformed from farmland in different years. Soil samples at 0.2 m depth increments were collected by a hollow-stem auger. Each sample was partitioned into two subsamples for the determination of soil water and other physicochemical properties.

The soil water and nitrate contents were respectively measured by oven drying and ion chromatography (ICS-1100). The ratios of water standardized by Z-Score to nitrate standardized by Z-Score were used to evaluate the coupling effects of water and nitrate. Although combined with isotope compositions (δ^2H-H_2O, δ^{18}O-H_2O, ^{3}H-H_2O, δ^{15}N-NO_3^-, and δ^{18}O-NO_3^-), the soil water and nitrate contents were used to explore recharge mechanism of soil water and legacy effects of nitrate in our previous studies (Ji et al., 2020; Ji et al., 2021). But this study emphasized the multivariate controls of water and nitrate in the deep loess deposits under different land use types.

Several physicochemical properties were also identified. Soil texture was determined by the sieve-pipette method. Magnetic susceptibility (MS) was measured via the magnetic susceptibility meter (MS2, Bartington, UK) and dual frequency sensor (MS2B) (Dearing, 1994; Liu et al., 2016). Soil pH and EC were measured by the pH/ion

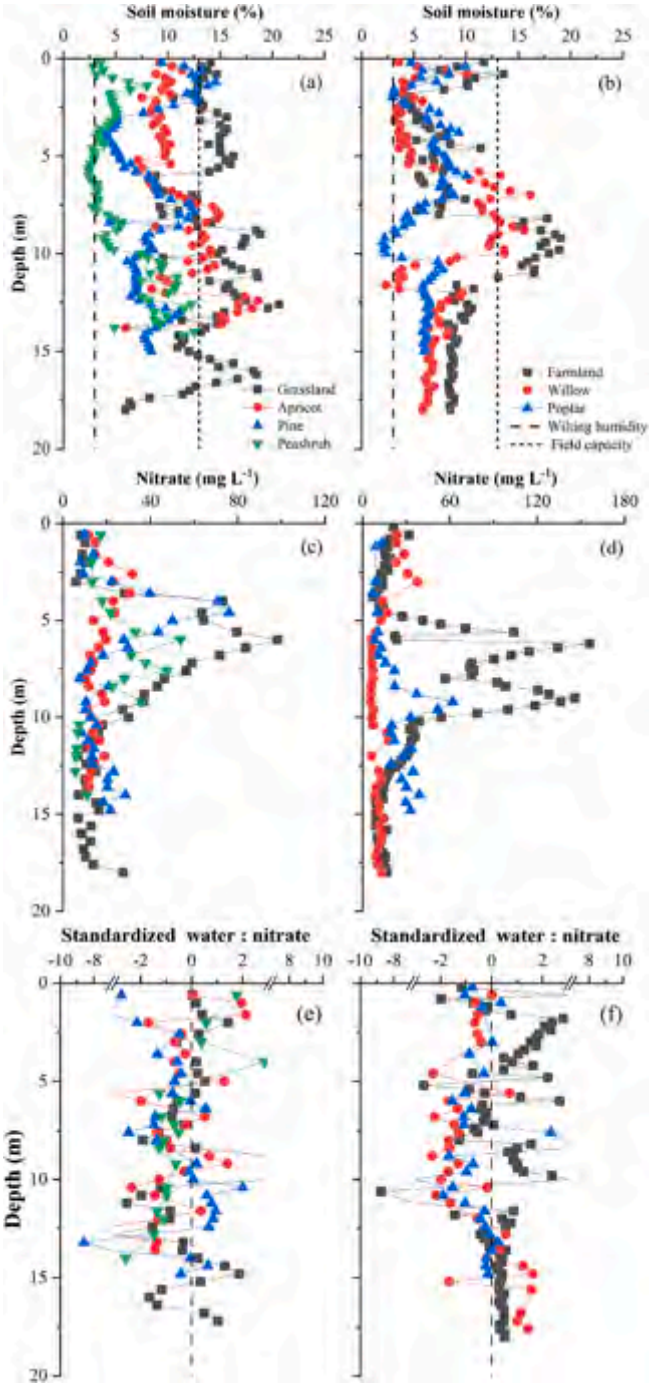

Fig. 2. Profiles of soil water, nitrate contents, and ratios of standardized water to standardized nitrate in SM (a&c&e) and DB (b&d&f). They respectively share the same legend.

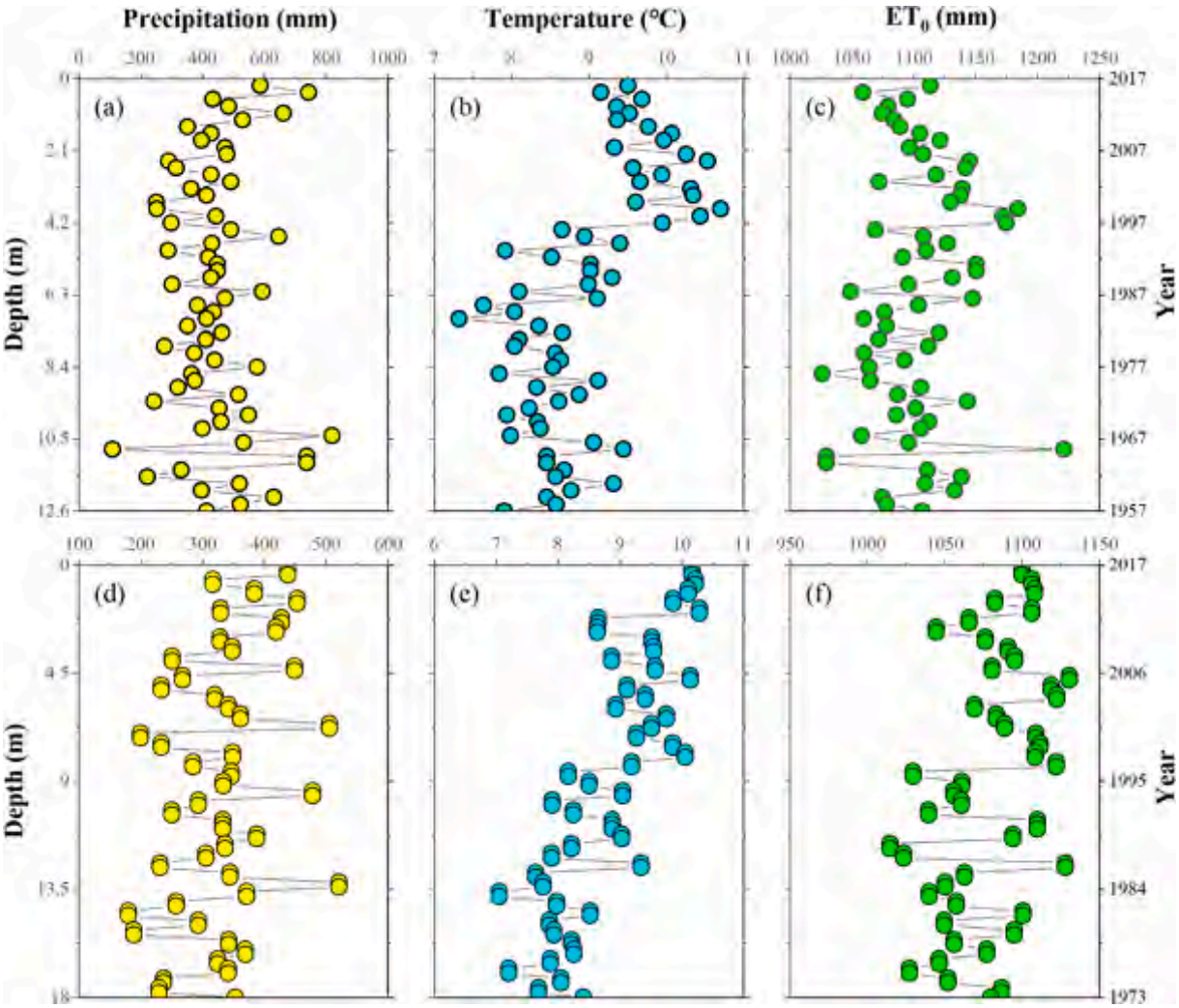

Fig. 3. Reconstructed precipitation, temperature, and ET_0 at different depths in SM (a−c) and DB (d−f). ET_0, potential evapotranspiration.

concentration/conductivity multi-parameter tester (SG78-FK-CN, Mettler Toledo, Switzerland). Soil organic carbon (SOC) was determined by dichromate oxidation method.

2.3. Combined effects of multiple environmental factors

Climatic factors and soil properties were both considered to discuss the possible combined effects because of their connections with soil water described below. Precipitation and ET_0 overall determine the inputs and outputs of soil water (Ye et al., 2019). Soil texture has significant impacts on water capacity and movement (Fang et al., 2016). Other soil properties and nutrient stoichiometry are responsible for N transformation processes (Lindsay et al., 2010; Yang et al., 2020). As such, precipitation, temperature, ET_0, soil texture, and MS were considered as potential factors controlling soil water variability, while soil water content (SWC), soil texture, MS, pH, EC, and SOC were selected as possible controlling factors for nitrate variability.

Soil properties were directly measured at each depth, so the climate-soil relationship at different depths could be established. Considering that soil water moved by piston flow, the soil water at different depths corresponded to precipitation in different years. The infiltration rate of 1963-precipitation was identified according to tritium peak (11 m and 22 m in SM and DB, data not shown). With estimated infiltration rates from tritium peak method, the ages of soil water at different depths were inversely calculated, and the historical climatic factors along the soil profiles were reconstructed. The monthly precipitation and temperature were collected from SM and DB weather stations during 1957–2017 from China Meteorological Administration, and the climate reconstruction results basically covered the > 13 m deep boreholes. The Hargreaves formula recommended by FAO was used to calculate ET_0 (Hargreaves. et al., 1994).

Partial correlation and bivariate wavelet coherence (BWC, n = 2) were both used to explore the best individual factor, while stepwise multiple linear regression (SMIR) and multiple wavelet coherence (MWC, n = 3 and 4) were both used to discuss the best multi-factor combination explaining variations under different land use types. The Monte Carlo method was used to obtain BWC and MWC at 95 % significance level (Hu and Si, 2016; Hu et al., 2017; Yang et al., 2021). The presentation of individual and multiple environmental factors were estimated via the average value of wavelet coherence (AWC) and percent area of significant coherence (PASC) of the total wavelet scale-depth domain (Hu and Si, 2016). The PASC values were mostly considered to select the best combination of environmental factors. Just PASC values > 5 % were considered as statistically significant, and an extra factor would not be considered significant unless PASC increased by at least 5 %. In addition, we divided the entire domain into three scales when explaining variations, i.e., small scales (< 2.5 m), medium scales (2.5–7.5 m), and large scales (> 7.5 m), respectively.

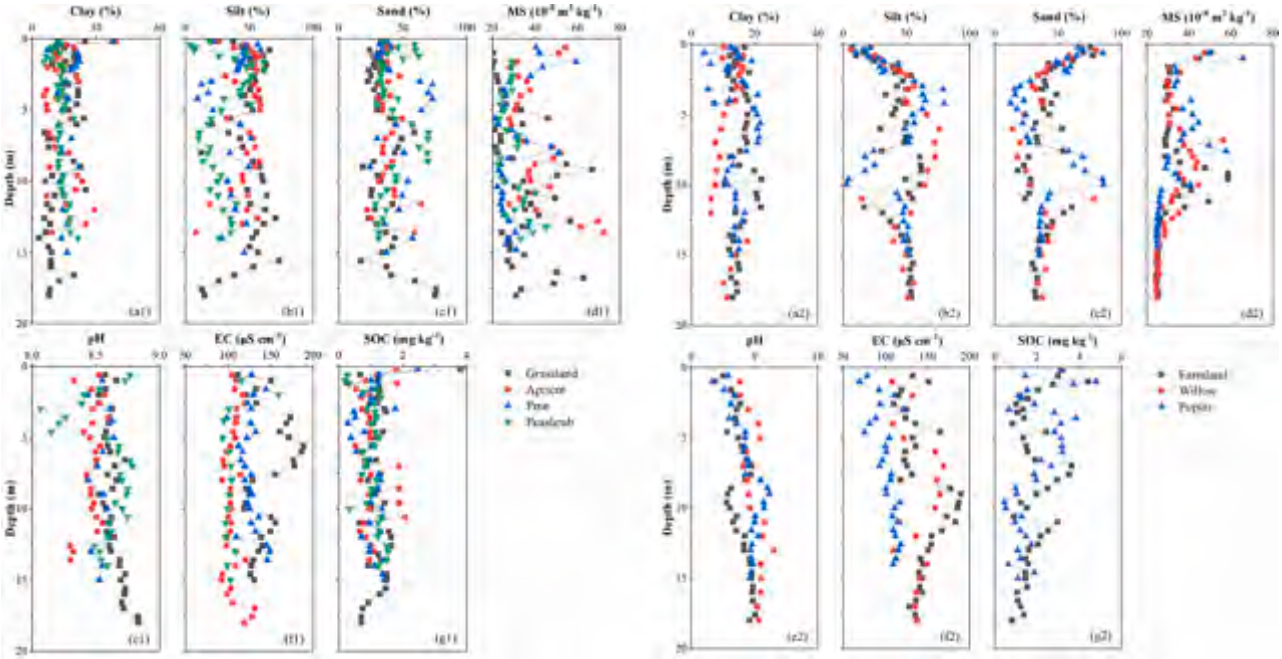

Fig. 4. Profiles of soil physicochemical properties under different land use types in SM (a1−g1) and DB (a2−g2). The SOC contents under willow were not measured because of the missing samples. MS, magnetic susceptibility; SOC, soil organic carbon.

3. Results

3.1. Soil water and nitrate variability

Soil water contents varied with vegetation types and soil depths (Fig. 2a&b). The water contents under shallow-rooted vegetation (grassland and farmland) were significantly higher than those of deep-rooted vegetation (apricot, pine, peashrub, willow, and poplar). Despite different vegetation types, the water contents overall declined with increasing tree ages. Particularly, the water contents within 10–15 m under older peashrub (35 years) were higher than those of younger pine (25 years) due to the shallow depth of root distribution with further results in less root water uptake. The water contents within 0–2 m drastically fluctuated, affected by the dual effects of precipitation and evapotranspiration. The lower water contents below 2 m suggested large root water uptake effects under deep-rooted shrubland and forestland (apricot, pine, peashrub, willow, and poplar, Fig. 2a&b). Despite lower water contents under deep-rooted vegetation, the water contents in paleosol layers (8–12 m) were relatively higher because of greater water retention capacity.

Similarly, nitrate contents also differed with vegetation types and soil depths (Fig. 2c&d). The nitrate contents under deep-rooted vegetation were relatively lower than those of farmland and grassland because of lower N fertilizer inputs. The nitrate contents under deep-rooted vegetation generally declined with tree ages, with several exceptions due to differences in root absorption and N fixation. For instance, despite lower fertilizer inputs, older peashrub had higher nitrate concentration than those of younger apricot and pine in SM due to the symbiotic N fixation of legumes and *Rhizobium*. The nitrate concentration showed a parabolic shape, with the peak depths ranging 2.6–9.2 m (Fig. 2c&d). The peak contents under grassland (98.2 mg L^{-1}) and farmland (156.0 mg L^{-1}) were significantly higher than those of deep-rooted vegetation (31.8–76.1 mg L^{-1}), with relatively larger peak depths (6 m for grassland and 6.2 m for farmland). The older plants usually had greater stabilized depths and concentration. Therefore, each profile was divided into two zones, i.e., high variation zone (high water deficit and nitrate accumulation within 0–10 m) and relative stabilization zone (low water deficit and nitrate accumulation below 10 m).

Further, the ratios of standardized water to standardized nitrate were 0.1 ± 1.8, −0.8 ± 1.7, −0.9 ± 2.0, −0.6 ± 1.3, 0.3 ± 1.7, −0.6 ± 1.2, and −0.5 ± 1.3 under different land use types (Fig. 2e&f). Obviously, the positive and negative ratios suggested synergistic and antagonistic relationships of water and nitrate under shallow- and deep-rooted plants, respectively. This phenomenon indicated that nitrate could move easily with soil water under shallow-rooted plants, while nitrate was easily retained in the soil under deep-rooted plants due to large water deficit. In addition, the standardized ratios in SM were highly variable across the entire profiles, while the ratios in DB largely fluctuated within 0–10 m, and tended to stabilize below 10 m (Fig. 2e&f). The results are consistent with soil water and nitrate profiles as described above (drastically fluctuated within 0–10 m and relatively stabilized below 10 m), and the ratios of standardized water to standardized nitrate can assess the coupling relationship between soil water and nitrate in soils as an important tool.

3.2. Variations of environmental factors

The precipitation and ET_0 in SM insignificantly increased during 1957–2017 ($p = 0.805$ and 0.451), with the trends of 2.9 mm $yr^{-1}$and 0.11 mm yr^{-1}, respectively. The temperature showed a significant upward trend ($p < 0.001$, Fig. S1), with the rate of 0.03 ℃ yr^{-1}. The precipitation was stabilized ($p = 0.361$), while the temperature and ET_0 showed a significant upward trend in DB ($p < 0.001$), with the increased rates of 3.7 mm yr^{-1}, 0.04 ℃ yr^{-1}, and 0.76 mm yr^{-1}, respectively (Fig. S1). After climate reconstruction in the thick unsaturated zones, the profiles within 0–12.6 m and 0–18 m in SM and DB corresponded to the climatic factors during 1957–2017 and 1973–2017, respectively. Precipitation, temperature, and ET_0 mostly declined with soil depths but increased with time (Fig. 3).

The soil texture under different land use types fluctuated widely within the top 0–1 m, and tended to stabilize within 1–5 m (Fig. 4a−c). But high variability was observed in the deep layers (below 5 m) with lower clay and higher sand contents. In particular, the silt and sand contents exhibited a complementary relationship, i.e., higher silt contents corresponded to lower sand contents. Except for the surface layers, the MS values were higher and more variable in the deep layers (below

Table 2
Partial correlation coefficients between soil water (nitrate) and environmental factors under different land use types.

Variable	Location	Land use	Environmental factors							
			Clay (%)	Silt (%)	Sand (%)	MS (10^{-8} m^3 kg^{-1})	P (mm)	T (℃)	ET_0 (mm)	
Soil water	SM	Grassland	0.17	0.19	0.09	**0.61****	**0.31***	−0.06	**0.30***	
		Apricot	0.18	0.17	0.15	**0.57****	−0.07	**−0.41****	0.10	
		Pine	−0.08	0.06	−0.14	**0.82****	−0.10	0.04	−0.08	
		Peashrub	−0.07	−0.18	**−0.42****	**0.47****	−0.03	−0.12	−0.18	
	DB	Farmland	−0.10	−0.09	−0.10	**0.79****	−0.10	**−0.45****	**0.26***	
		Willow	0.01	0.01	−0.01	**0.77****	−0.18	**−0.51****	0.06	
		Poplar	**−0.24***	**−0.25***	**−0.26***	**0.29***	−0.04	−0.16	0.20	
Variable	Location	Land use	Environmental factors							
			SWC (%)	Clay (%)	Silt (%)	Sand (%)	MS (10^{-8} m^3 kg^{-1})	pH	EC (μs cm^{-1})	SOC (mg kg^{-1})
Nitrate	SM	Grassland	0.05	0.08	0.04	0.09	−0.05	**−0.40****	**−0.49****	**−0.25***
		Apricot	**−0.28***	−0.08	−0.05	−0.13	−0.12	0.13	−0.14	**−0.28***
		Pine	−0.09	0.01	−0.11	−0.01	0.07	−0.04	−0.24	**−0.49****
		Peashrub	**−0.69****	**0.29***	0.10	**0.40***	−0.03	0.22	**0.26***	−0.11
	DB	Farmland	0.00	0.03	−0.01	−0.04	**0.41****	0.20	−0.18	**0.37****
		Willow	**−0.38****	0.02	−0.02	−0.02	0.02	**−0.56****	**−0.31****	–
		Poplar	0.06	0.04	0.05	0.05	0.14	**0.56****	**−0.42****	0.02

The bold environmental factors were significantly correlated with soil water and nitrate. And the environmental factors, with the highest correlation coefficients under each land use type, were marked in bold and underlined. P, precipitation; T, temperature; ET_0, potential evapotranspiration; SWC, soil water content; MS, magnetic susceptibility; SOC, soil organic carbon. **Correlation significant at $p < 0.01$ (two-tailed); *Correlation significant at $p < 0.05$ (two-tailed).

Table 3
Wavelet coherence between soil water (nitrate) and environmental factors under different land use types.

Variable	Location	Land use	Factor	AWC	PASC (%)	Variable	Location	Land use	Factor	AWC	PASC (%)
Soil water	SM	Grassland	**Sand**	**0.60**	**44**	Nitrate	SM	Grassland	EC	0.32	6
			Silt-Sand	0.77	38				SWC-EC	0.65	16
			Clay-Sand-ET_0	0.86	34				**SWC-pH-EC**	**0.79**	**22**
		Apricot	Sand	0.54	29			Apricot	SOC	0.38	14
			Sand-MS	**0.71**	**43**				**EC-SOC**	**0.67**	**21**
			Silt-Sand-MS	0.83	42				SWC-EC-SOC	0.83	24
		Pine	MS	0.51	29			Pine	SOC	0.31	7
			Silt-MS	**0.77**	**45**				**Silt-SOC**	**0.66**	**22**
			Clay-Silt-MS	0.86	43				Silt-MS-SOC	0.80	25
		Peashrub	**MS**	**0.48**	**17**			Peashrub	SOC	0.42	22
			Sand-MS	0.67	17				SWC-MS	0.63	22
			Silt-Sand-MS	0.81	21				**SWC-Sand-MS**	**0.81**	**39**
	DB	Farmland	MS	0.50	29		DB	Farmland	MS	0.33	12
			Sand-MS	**0.78**	**37**				MS-EC	0.56	15
			Sand-MS-T	0.87	41				**MS-EC-SOC**	**0.76**	**21**
		Willow	Sand	0.45	21			Willow	**pH**	**0.46**	**31**
			Sand-MS	**0.77**	**44**				Clay-pH	0.69	32
			Sand-MS-T	0.87	48				MS-pH-EC	0.79	32
		Poplar	Sand	0.48	28			Poplar	pH	0.46	21
			Sand-MS	0.76	41				**SWC-pH**	**0.72**	**39**
			Sand-MS-ET_0	**0.87**	**47**				SWC-Clay-pH	0.81	43

The PASC values were used to select the best combination of environmental factors. Just PASC values > 5% were considered as statistically significant, and an extra factor would not be considered significant unless PASC increased by at least 5 %. The environmental factors, most significantly correlated with soil water and nitrate under each land use type, were marked in bold and underlined. ET_0, potential evapotranspiration; T, temperature; SWC, soil water content; MS, magnetic susceptibility; SOC, soil organic carbon.

5 m, Fig. 4d), suggesting the difficulties of water and solute transport. The pH values suggested that the soils under different land use types were alkaline, which slightly increased with soil depths (Fig. 4e). With relatively higher EC values under shallow-rooted plants, the EC profiles were highly variable under different land use types (Fig. 4f). Additionally, the SOC values in SM sharply decreased within the top 0–1 m, and tended to stabilize below 1 m. The SOC values in DB declined with soil depths, with fluctuation in the deep layers under farmland and poplar (Fig. 4g).

3.3. Individual factor explaining soil water and nitrate variations

The soil water contents under different land use types were positively correlated with MS, with the correlation coefficients ranging 0.29–0.82 ($p < 0.01$, Table 2). In addition, temperature significantly influenced soil moisture under apricot, farmland, and willow ($p < 0.01$, Table 2). And the soil water contents under shallow-rooted plants (grassland and farmland) were positively correlated with ET_0 ($p < 0.05$, Table 2). According to wavelet analysis, the best individual factor under each land use type was Sand and/or MS, with the AWC and PASC values ranging 0.45–0.60 and 17 %–44 % (Table 3). The coherence mostly exhibited at large scales (> 7.5 m) followed by medium scales (2.5–7.5 m). Sand exhibited out-of-phase coherence (negative correlation) with soil water, while MS performed in-phase coherence (positive correlation) with soil water at almost all depths (Fig. 5). Overall, soil texture rather than climatic factors dominated soil water variability, and MS was the most important factor.

The nitrate concentration under each land use type was simultaneously related to multiple soil physiochemical properties ($p < 0.05$, Table 2). The best factors explaining nitrate variability under different land use types were EC, SWC, SOC, MS, and/or pH, with the correlation coefficients ranging from −0.69 to 0.56 (Table 2). According to wavelet analysis, the best individual factor under each land use type was EC, SOC, MS, and/or pH (Fig. 5), with the AWC and PASC values ranging

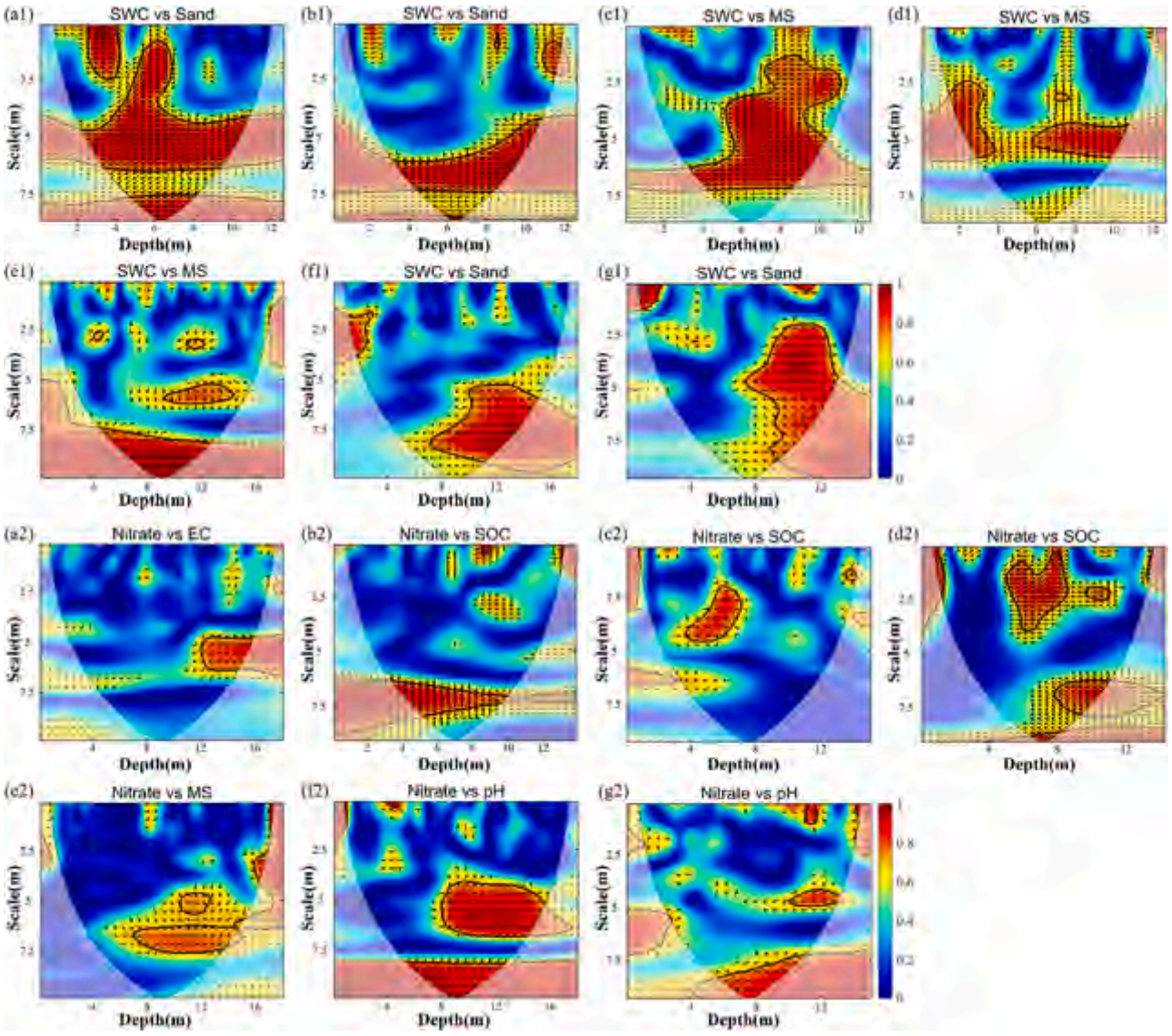

Fig. 5. Bivariate wavelet coherency between soil water (nitrate) and environmental factors under grassland (a), apricot (b), pine (c), peashrub (d), farmland (e), willow (f), and poplar (g), respectively. The horizontal axis is the soil depth below the ground. Arrows show the phase angles of the wavelet spectra. The right arrows indicate positive relationships and the left arrows indicate negative relationships. Thin solid lines demarcate the cones of influence and thick solid lines show the 95 % confidence levels. MS, magnetic susceptibility; SOC, soil organic carbon.

0.31–0.46 and 6 %–31 %. The coherence also exhibited at large scales (> 7.5 m) followed by medium scales (2.5–7.5 m). MS exhibited out-of-phase coherence (negative correlation) with nitrate, while EC, SOC, and pH exhibited in-phase coherence (positive correlation) with nitrate at almost all depths (Table 3). Overall, SWC, pH, EC, and SOC were the most important factors.

3.4. Multiple factors jointly controlling soil water and nitrate variations

The soil water variability was mostly explained by Sand-MS-T-Silt-ET_0 (Table 4), which explained 39 %–87 % under different land use types. The best two-factor combination was Sand-MS (Fig. 6). The AWC and PASC values ranged 0.67–0.78 and 17 %–45 %, and increased by 0.17–0.32 and −6 %–23 % compared with the single factors (Table 3). The coherence was mostly observed at large scales (> 7.5 m) and almost all depths. Further, the best three-factor combination was Silt-Sand-MS (Fig. S2). The AWC and PASC values ranged 0.81–0.87 and 21 %–48 %, and were improved by 0.09–0.14 and −4 %–6 % compared with the two-factor combination (Table 3). The environmental factors mostly contributed to soil water variability at medium (2.5–7.5 m) and large scales (> 7.5 m).

The nitrate variability under each land use type was greatly explained by EC-pH-SOC-SWC-Sand, with the adjusted R^2 ranging 0.31–0.82 (Table 4). Further, the best two-factor combination was SWC-EC (Fig. 6) with the AWC and PASC values ranging 0.56–0.72 and 15 %–39 % (Table 3). The AWC and PASC values increased by 0.21–0.35 and 0–18 % compared with the single factors, mostly contributed by medium (2.5–7.5 m) and large scales (> 7.5 m, $p < 0.05$). These factors explained nitrate variability at almost all depths. The best three-factor combination was SWC-MS-EC (Fig. S2). The AWC and PASC values ranged 0.76–0.83 and 21 %–43 %, and increased by 0.09–0.20 and 0–17 % compared with the two-factor combination (Table 3).

4. Discussion

4.1. How do soil water and nitrate contents relate to land use?

The plantation of deep-rooted plants greatly reduced soil water

Table 4
Stepwise multiple linear regression between soil water (nitrate) and environmental factors under different land use types.

Variable	Location	Land use	Function (Standardized regression coefficients)	F	Adjusted R^2
Soil water	SM	Grassland	SWC = -0.58*Sand + 0.48*MS	74.66	0.70
		Apricot	SWC = 0.61*MS - 0.30*T	35.42	0.53
		Pine	SWC = 0.67*MS + 0.47*Silt	211.77	0.87
		Peashrub	SWC = 0.45*MS - 0.38*Sand - 0.29*ET_0	14.13	0.39
	DB	Farmland	SWC = 0.86*MS - 0.25*Sand - 0.58*T + 0.30*ET_0	56.18	0.71
		Willow	SWC = 0.46*Silt + 0.80*MS - 0.50*T - 0.12*P	68.60	0.75
		Poplar	SWC = -1.96*Sand - 1.28* Silt + 0.22*MS	38.89	0.61
Variable	Location	Land use	Function (Standardized regression coefficients)	F	Adjusted R^2
Nitrate	SM	Grassland	Nitrate = -0.61*Silt - 0.44*EC - 0.37*pH - 0.22*SOC	17.84	0.43
		Apricot	Nitrate = -0.43*SWC + 0.27*Silt - 0.24*SOC	10.97	0.31
		Pine	Nitrate = 0.56*Sand - 0.34*SOC	52.08	0.58
		Peashrub	Nitrate = -0.65*SWC + 0.50*Sand + 0.18*EC + 0.16*Clay	51.72	0.74
	DB	Farmland	Nitrate = 0.77*MS - 0.53*Sand + 0.37*SOC - 0.24*EC + 0.29*pH	17.50	0.48
		Willow	Nitrate = -0.36*EC - 0.51*pH - 0.44*SWC + 0.22*Clay	103.22	0.82
		Poplar	Nitrate = 0.63*pH - 0.56*EC + 0.17*MS	54.63	0.69

P, precipitation; T, temperature; ET_0, potential evapotranspiration; SWC, soil water content; MS, magnetic susceptibility; SOC, soil organic carbon.

contents (Fig. 2a&b), with the relative water deficit of 1249 mm and 646 mm in SM and DB, respectively. The variations of soil water over time and depths were evaluated by tree ages (i.e., space for time). The water contents within 0–10 m gradually decreased from 1982 to 2017 in SM and from 1967 to 2017 in DB, with the exception of the middle 0–4 m in DB (Fig. 7a&c). The phenomenon could be attributed to shallow depths of water consumption under willow compared to poplar. The water deficit under deep-rooted plants are closely correlated to large root water uptake effects (Shi et al., 2021a; Tao et al., 2021). The older the trees, the higher the root biomass and transpiration effects (Li et al., 2019b; Li et al., 2016; Li et al., 2017). Plant roots easily extend to deep soils (usually > 10 m) in regions with seasonally arid climate and higher permeability (Li et al., 2019a). As such, water deficit mostly occurs in deep soils, which potentially reduces or even prevents groundwater recharge (Huang et al., 2019; Li et al., 2018; Zhang et al., 2018), especially in those regions with thick vadose zones, limited recharge rates, and deep-rooted plants (Gates et al., 2011; Li and Si, 2018; Lin and Wei, 2006). Despite lower rainfall in DB (332 mm) relative to SM (437 mm), the higher recharge rates in DB, indicated by tritium peak depths, were ascribed to the higher sand contents and lower matric suction (Table 5), which also confirmed the dominance of soil texture on water infiltration.

Different degrees of residual nitrate were presented in the thick loess deposits after the transformation from grassland/farmland to non-fertilized forestlands and shrublands (Fig. 2c&d). In this study, higher tree ages usually indicated lower fertilizer inputs and higher root uptake under forestlands and shrublands. Therefore, the lower nitrification of synthetic fertilizer applied before land use change and higher assimilation of vegetation (ammonium and nitrate were converted into organic compounds, i.e. amino acids and proteins.) both contributed to the lower nitrate contents under non-fertilized lands (Ji et al., 2020). Similarly, the nitrate contents within 0–10 m were assessed from 1982 to 2017 in SM and from 1967 to 2017 in DB (Fig. 7b&d). Obviously, the existence of residual nitrate suggested that the synthetic fertilizer may be retained for 50 years in the deep unsaturated zones (Ji et al., 2020); that is to say, N inputs (organic amendments, fixation, and deposition) were chronically greater than N outputs (root absorption, gaseous emissions, and leaching) (Scanlon et al., 2008; Yang et al., 2020). Nitrate leaching is still an important pathway for N loss on the Loess Plateau. With the dominance of recharge rates on nitrate leakage (Huang et al., 2018; Ji et al., 2021), the travel time of nitrate ranges between decades and centuries in those regions with low recharge rates and deep unsaturated zones (Kaandorp et al., 2021; Turkeltaub et al., 2018).

4.2. *How do multiple environmental factors combine to control soil water and nitrate?*

With the sampling depths ranging 13.8–18 m below the surface, the deep soil water and nitrate reservoirs obviously varied with multiple environmental factors, which were identified by both classical statistics (partial correlation and SMIR, Table 2&4) and wavelet analysis (BWC and MWC, Table 3). The results of wavelet analysis were overall consistent with those of classical statistics, but could identify the combined effects of environmental factors at different depths and scales (Hu et al., 2017; Lu et al., 2019; Mihanović et al., 2009). Therefore, it is essential to explore the multivariate controls of water and nitrate in deep loess deposits by multiple methods.

Specifically, the deep soil water reservoirs were individually or simultaneously influenced by sand and MS (Tables 2–4). First, it is easier for soil water to infiltrate downwards in coarse-textured soils with higher sand contents (35.7 %–44.5 %) due to the lower water retention capacity (Table 5). For instance, the 1963-precipitation in SM and DB has respectively moved approximately 11 m and 22 m in the past 54 years, which is obviously deeper than reported for loess tablelands which had higher rainfall and fine-textured soils (Huang et al., 2020; Huang et al., 2019; Li and Si, 2018).

Second, as the important agent to characterize soil particle sizes, MS was the key factor to explain the variations of SBD and deep soil water within 3–13 m (Lu et al., 2019). Theoretically, the finer the particle sizes, the larger the MS values (Shi et al., 2021b). In this study, the paleosol layers with finer particle sizes and higher water contents had higher MS values (Fig. 2&4). Although particle size distribution is usually used to evaluate soil hydraulic properties (Yang et al., 2020), MS may be more superior to characterize soil water variability in thick loess deposits due to its sensitivity to pedogenic factors and climate parameters (Jordanova and Jordanova, 2021). Alternatively, MS could substitute soil texture as the ideal indicator of soil water because of the convenience of measurement process and accuracy of measurement results in the future. Overall, sand and MS were mostly responsible for the variability of deep soil water due to their interactions on water permeability and retention.

Additionally, the deep nitrate reservoirs were mostly controlled by SWC, pH, EC, and SOC (Tables 2–4). First, soil water, controlled by soil particle sizes and MS, significantly influences nitrate transport processes in soils. The nitrate leaching rates are negatively correlated to clay and silt contents (Gao et al., 2021). Further, soil water also affects aeration and redox potential, which remarkably regulates nitrate transformation

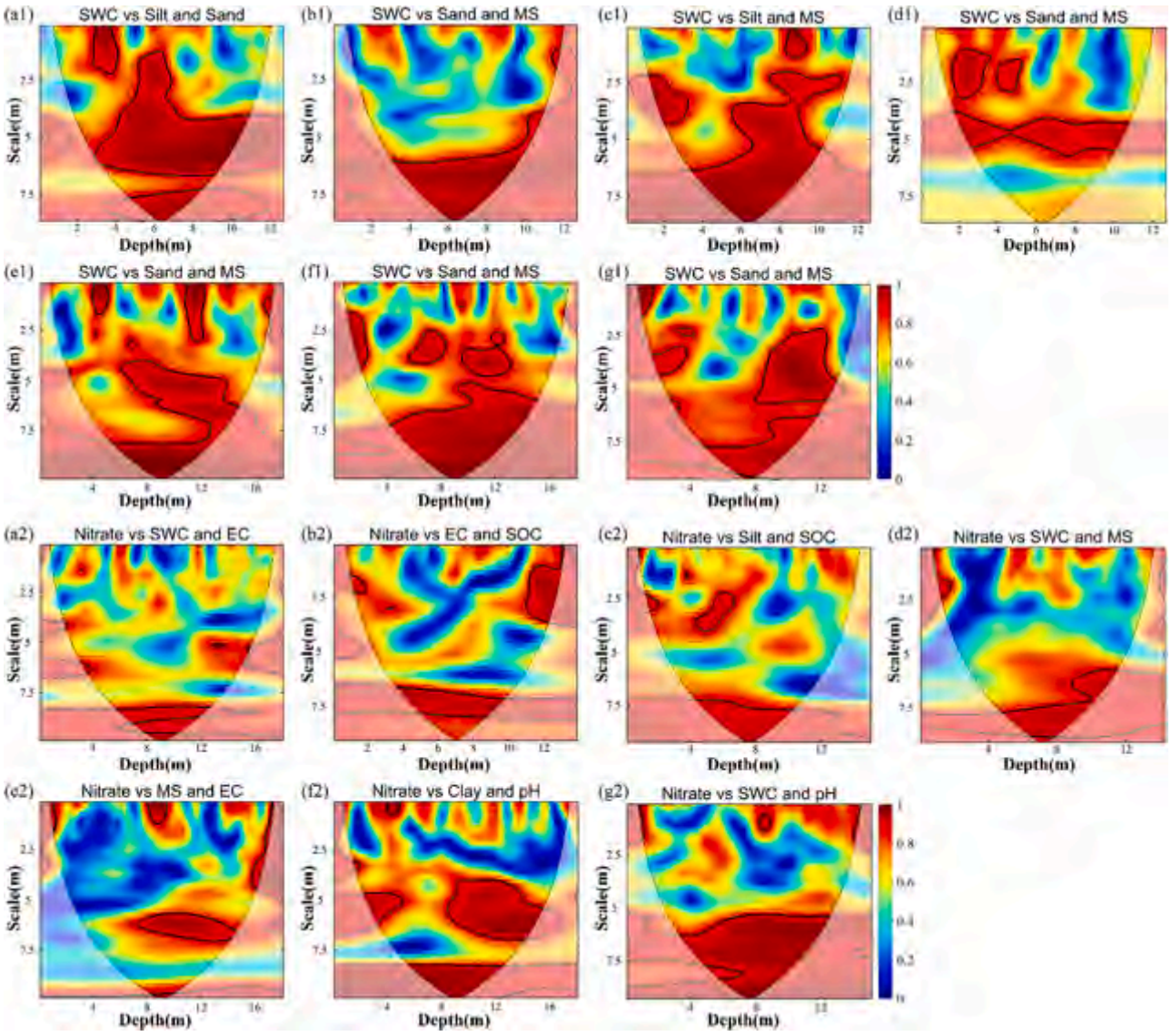

Fig. 6. Multiple wavelet coherency (n = 3) between soil water (nitrate) and environmental factors under grassland (a), apricot (b), pine (c), peashrub (d), farmland (e), willow (f), and poplar (g), respectively. The horizontal axis is the soil depth below the ground. Thin solid lines demarcate the cones of influence and thick solid lines show the 95 % confidence levels. SWC, soil water content; MS, magnetic susceptibility; SOC, soil organic carbon.

processes (Cui et al., 2020). For instance, higher soil water facilitates the occurrence of denitrification and ammonia volatilization (Sigler et al., 2020). It is difficult for nitrate to transport and transformation in deep loess deposits with large water deficit (Fig. 2). Second, the number of positive charges (H^+) on the soil surface decreases with increases pH values (Yang et al., 2020). Despite electrostatic attraction of H^+ and NO_3^--N, nitrate was more leachable in the alkaline loess (8.5–9.0, Table 5), especially for deep soils with higher pH values (Fig. 4). Third, as an essential indicator of soil salinity, the EC values are closely correlated to climate, fertilization, and soil texture. In this study, the saline-alkali soil in northern Shaanxi had high salinity (Table 5), which could destroy soil structure, reduce soil aeration, and further restrain the occurrence of N transformation processes. Finally, the surface-aggregated SOC provided essential substrate and energy for N biogeochemical processes (Fig. 4), with the carbon–nitrogen coupling relationship in soils (Deng et al., 2016; Lu et al., 2021; Tashi et al., 2016).

In this study region, we used nitrate contents and isotope compositions to explore the legacy effects and potential sources (Ji et al., 2020). Specifically, nitrification and mineralization largely contribute to soil nitrate reservoirs on the Loess Plateau, with the limited denitrification in deep loess deposits (Ji et al., 2020). Considering the predominant nitrification process, ammonium in urea-based fertilizer is quickly oxidized to NO_3^--N under less udic moisture regime because of oxygen partial pressure variations, and the nitrifying bacteria activities are also controlled by pH and SOC (Elrys et al., 2021b). The mineralization of converting organic N to ammonium, which provides an essential substrate for nitrification, is positively affected by soil water and carbon contents, but negatively influenced by pH (Elrys et al., 2021a). Finer soil particles and favorable water contents promote the occurrence of mineralization and nitrification processes (Scanlon et al., 2008). Denitrification is the critical means to remove residual nitrate in soils. The activity of heterotrophic denitrifying microorganisms is lower with limited soil water and organic carbon contents (Barkle et al., 2007; Ji et al., 2020). Nitrification, mineralization, and denitrification are suppressed in soils with high salinity. The abundances of different functional genes (*amoA*-AOA, *amoA*-AOB, *chiA*, *nifH*, *nirS*, *nirK*, and *nosZ*) are also affected by multiple environmental factors at different depths and scales (Kuypers et al., 2018; Levy-Booth et al., 2014; Lindsay et al., 2010; Xia et al., 2011), which needs to be further explored by microbial approaches, i.e., PCR quantification, high-throughput sequencing, and

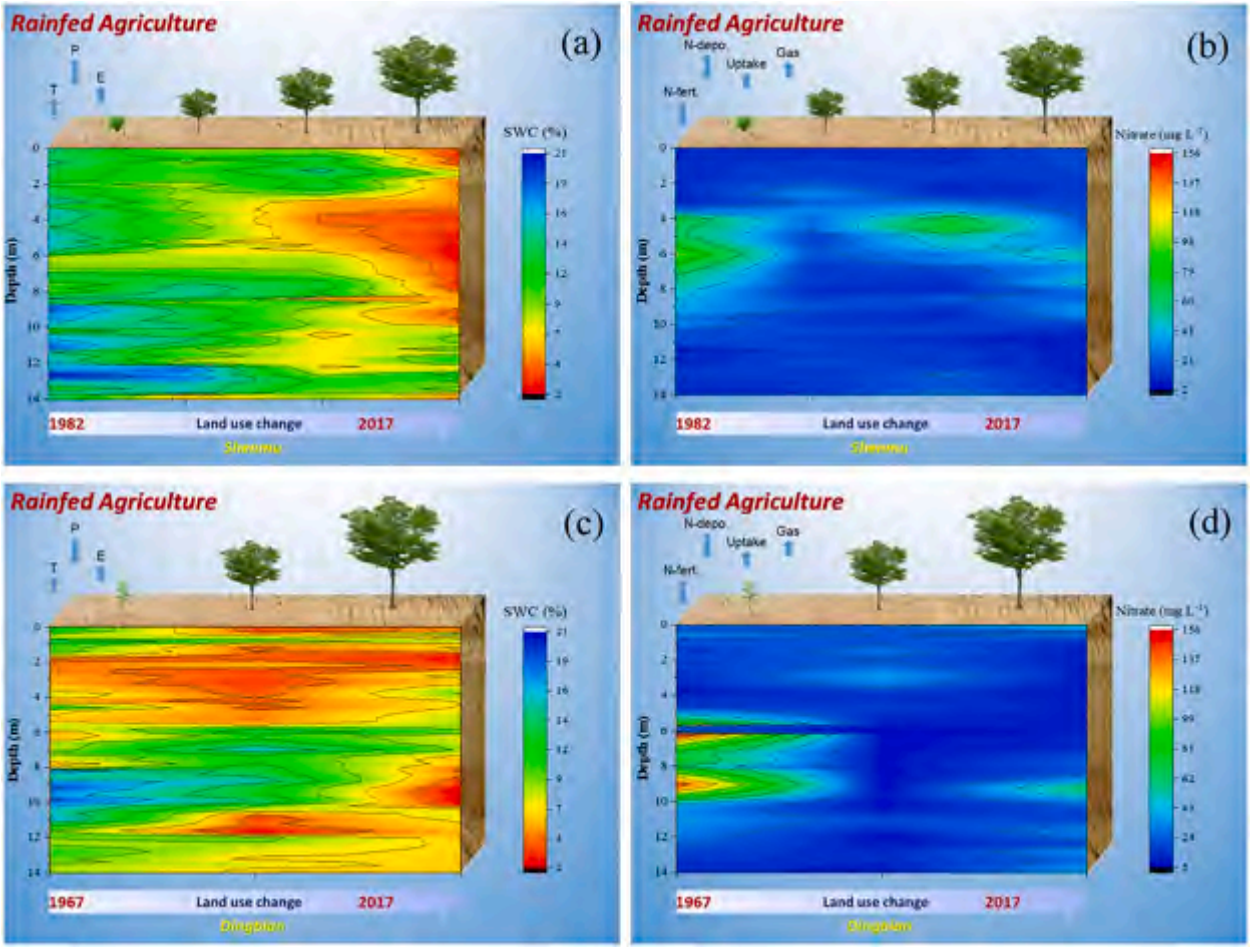

Fig. 7. Variations of soil water and nitrate contents in SM (a&b) and DB (c&d) over time and depths. Despite different vegetation types, the time axis was estimated with tree ages (i.e., space for time). The effects of land use conversion on deep soil water and nitrate reservoirs were explored at both temporal and spatial scales. P, precipitation; T, temperature; E, evaporation.

Table 5
Main statistics of soil water, nitrate, and soil physicochemical properties.

Location	Land use	SWC (%)	Nitrate (mg L^{-1})	Clay (%)	Silt (%)	Sand (%)	MS (10^{-8} m^3 kg^{-1})	pH	EC (μs cm^{-1})	SOC (mg kg^{-1})
SM	Grassland	13.8 ± 3.0a	28.6 ± 25.7a	14.6 ± 7.6ab	49.2 ± 14.3a	35.7 ± 13.1b	33.8 ± 12.4b	8.6 ± 0.1a	106.4 ± 9.4b	1.2 ± 0.5a
	Apricot	11.2 ± 2.9b	16.6 ± 5.4b	14.6 ± 7.7ab	46.8 ± 11.8a	37.5 ± 8.4b	43.1 ± 19.4a	8.5 ± 0.1c	130.5 ± 23.1a	1.1 ± 0.4a
	Pine	8.5 ± 2.6c	22.3 ± 11.0ab	17.1 ± 5.8a	37.8 ± 13.4b	44.5 ± 14.6a	30.7 ± 9.2b	8.6 ± 0.1b	105.4 ± 15.9b	1.1 ± 0.4a
	Peashrub	5.7 ± 2.9d	21.9 ± 14.7ab	13.3 ± 3.9b	31.0 ± 15.6c	43.4 ± 13.4a	28.2 ± 7.1b	8.6 ± 0.2ab	101.9 ± 13.6b	1.1 ± 0.6a
DB	Farmland	9.6 ± 3.8a	39.1 ± 39.0a	15.3 ± 3.2a	42.8 ± 14.1a	41.7 ± 14.1a	32.5 ± 9.1a	8.8 ± 0.2b	144.3 ± 21.8a	1.9 ± 0.9a
	Willow	7.5 ± 3.5b	12.8 ± 7.6b	12.1 ± 3.4b	47.1 ± 17.6a	40.5 ± 16.8a	32.9 ± 7.4a	9.0 ± 0.1a	137.2 ± 20.1a	–
	Poplar	6.1 ± 1.9c	24.5 ± 13.1b	14.4 ± 4.5a	41.4 ± 19.4a	44.1 ± 20.9a	43.3 ± 45.5a	8.9 ± 0.2b	145.3 ± 22.5a	1.9 ± 1.1a

SWC, soil water content; MS, magnetic susceptibility; SOC, soil organic carbon. Different lowercase letters indicate significant differences ($p < 0.05$); however, if there are the same lowercase letters, there is no significant difference.

metagenomics.

4.3. What are the implications for vegetation and environmental management?

The conversion from grassland/farmland to non-fertilized forestlands and shrublands resulted in lower water storage, recharge rates, and nitrate leakage. And this decrease was larger with stand ages of deep-rooted plants (Huang et al., 2019; Huang et al., 2021). Particularly, nitrate could still be observed in soils even after 50 years without fertilization. Therefore, effective countermeasures should be taken for the sustainability of vegetation and environment. First, the deep-rooted plants with high water deficit should be removed or converted to new vegetation with low root water uptake in an appropriate age (Ji et al.,

2021). Alternatively, adjusting vegetation density and mixed (integrated) cultivation are good options to conserve soil water.

Second, considering the potential risk of nitrate contamination to groundwater, more attention should be paid to the removal of residual nitrate in deep unsaturated zones. Laboratory experiments have showed that the combined amendment of electric potential and biochar (Yuan et al., 2020), addition of zero-valent iron nanoparticles (Gibert et al., 2021), and application of electro-bioremediation (Choi et al., 2009) greatly remove nitrate from the soil. But their applicability on the Loess Plateau, in terms of operability and economy, needs to be carefully considered in the future. Furthermore, the identified multivariate controls of deep soil water (MS and sand) and nitrate (SWC, pH, EC, and SOC) are critical for developing scale- and depth- dependent simulation for downscaling and/or upscaling, with less labor and time. This study benefits the parameterizing of hydrological and biogeochemical models, especially in the deep unsaturated zones.

5. Conclusion

Understanding multivariate controls of soil water and nitrate in the deep unsaturated zones is essential to the sustainability of vegetation and environment. Thus, this study explored this issue by analyzing the wavelet coherence of soil water (nitrate) with climatic factors and soil properties. Large water deficit and low nitrate accumulation were observed within 0–10 m under non-fertilized forestlands and shrublands, with negative ratios of standardized water to standardized nitrate. Specifically, MS and sand were the most important influencing factors for soil water movement, while SWC, pH, EC, and SOC were individually or simultaneously responsible for nitrate transport and transformation, especially at large scales ($>$ 7.5 m). This study promotes the accurate estimation of process-based hydrological and biogeochemical models at regional or global scales, especially in the deep unsaturated zones.

CRediT authorship contribution statement

Wangjia Ji: Conceptualization, Writing – original draft, Investigation, Methodology, Writing – review & editing. **Yanan Huang:** Methodology, Writing – review & editing. **Bingbing Li:** Methodology, Writing – review & editing. **Zhi Li:** Conceptualization, Funding acquisition, Writing – review & editing, Supervision, Methodology.

Declaration of Competing Interest

The authors declare that they have no known competing financial interests or personal relationships that could have appeared to influence the work reported in this paper.

Data availability

Data will be made available on request.

Acknowledgements

This study is jointly funded by National Natural Science Foundation of China (42071043) and Chinese Universities Scientific Fund (2452020002).

Appendix A. Supplementary data

Supplementary data to this article can be found online at https://doi.org/10.1016/j.jhydrol.2022.128409.

References

Allison, G., Hughes, M., 1983. The use of natural tracers as indicators of soil-water movement in a temperate semi-arid region. J. Hydrol. 60, 157–173.
Barkle, G., Clough, T., Stenger, R., 2007. Denitrification capacity in the vadose zone at three sites in the Lake Taupo catchment, New Zealand. Soil Research 45 (2). https://doi.org/10.1071/sr06141.
Chen, Y., et al., 2015. Balancing green and grain trade. Nat. Geosci. 8 (10), 739–741.
Choi, J.H., Maruthamuthu, S., Lee, H.G., Ha, T.H., Bae, J.H., 2009. Nitrate removal by electro-bioremediation technology in Korean soil. J. Hazard. Mater. 168 (2–3), 1208–1216. https://doi.org/10.1016/j.jhazmat.2009.02.162.
Cui, Y., et al., 2020. Soil moisture mediates microbial carbon and phosphorus metabolism during vegetation succession in a semiarid region. Soil Biol. Biochem. 147 https://doi.org/10.1016/j.soilbio.2020.107814.
Dearing, J.A., 1994. Environmental magnetic susceptibility: using the Bartington MS2 system. Chi Pub.
Dekker, S.C., Rietkerk, M.A.X., Bierkens, M.F.P., 2007. Coupling microscale vegetation? soil water and macroscale vegetation?precipitation feedbacks in semiarid ecosystems. Glob. Change Biol. 13 (3), 671–678. https://doi.org/10.1111/j.1365-2486.2007.01327.x.
Deng, L., Wang, G.-L., Liu, G.-B., Shangguan, Z.-P., 2016. Effects of age and land-use changes on soil carbon and nitrogen sequestrations following cropland abandonment on the Loess Plateau, China. Ecol. Eng. 90, 105–112. https://doi.org/10.1016/j.ecoleng.2016.01.086.
Elrys, A.S., et al., 2021a. Patterns and drivers of global gross nitrogen mineralization in soils. Glob Chang Biol 27 (22), 5950–5962. https://doi.org/10.1111/gcb.15851.
Elrys, A.S., et al., 2021b. Global gross nitrification rates are dominantly driven by soil carbon-to-nitrogen stoichiometry and total nitrogen. Glob Chang Bio. 27 (24), 6512–6524. https://doi.org/10.1111/gcb.15883.
Fan, J., Hao, M., Malhi, S.S., 2010. Accumulation of nitrate N in the soil profile and its implications for the environment under dryland agriculture in northern China: A review. Can. J. Soil Sci. 90 (3), 429–440. https://doi.org/10.4141/cjss09105.
Fang, X., et al., 2016. Variations of deep soil moisture under different vegetation types and influencing factors in a watershed of the Loess Plateau. China. Hydrol. Earth Syst. Sci. 20, 3309–3323. https://doi.org/10.5194/hess-20-3309-2016.
Fu, B., et al., 2017. Hydrogeomorphic Ecosystem Responses to Natural and Anthropogenic Changes in the Loess Plateau of China. Annu. Rev. Earth Planet. Sci. 45 (1), 223–243. https://doi.org/10.1146/annurev-earth-063016-020552.
Gao, J., et al., 2021. High Nitrate Accumulation in the Vadose Zone after Land-Use Change from Croplands to Orchards. Environ. Sci. Technol. https://doi.org/10.1021/acs.est.0c06730.
Gao, J., Lu, Y., Chen, Z., Wang, L., Zhou, J., 2019. Land-use change from cropland to orchard leads to high nitrate accumulation in the soils of a small catchment. Land Degrad. Dev. 30 (17), 2150–2161. https://doi.org/10.1002/ldr.3412.
Gates, J.B., Scanlon, B.R., Mu, X., Zhang, L., 2011. Impacts of soil conservation on groundwater recharge in the semi-arid Loess Plateau. China. Hydrogeology Journal 19 (4), 865–875. https://doi.org/10.1007/s10040-011-0716-3.
Gee, G.W., Hillel, D., 2006. Groundwater recharge in arid regions: Review and critique of estimation methods . Hydrol. Process. 2 (3), 255–266.
Gibert, O., et al., 2021. Removal of nitrate from groundwater by nano-scale zero-valent iron injection pulses in continuous-flow packed soil columns. Sci. Total Environ. 810, 152300 https://doi.org/10.1016/j.scitotenv.2021.152300.
Gu, X., Jamshidi, S., Sun, H., Niyogi, D., 2021. Identifying multivariate controls of soil moisture variations using multiple wavelet coherence in the U.S. Midwest. Journal of Hydrology 602. https://doi.org/10.1016/j.jhydrol.2021.126755.
Han, X., et al., 2019. Effects of plantation age and precipitation gradient on soil carbon and nitrogen changes following afforestation in the Chinese Loess Plateau. Land Degrad. Dev. 30 (18), 2298–2310. https://doi.org/10.1002/ldr.3422.
Hargreaves, G.H., Fellow, ASCE, 1994. Defining and using reference evapotranspiration. J. Irrig. Drain. Eng., 120: 1132–1139.
Hu, W., Si, B.C., 2016. Technical note: Multiple wavelet coherence for untangling scale-specific and localized multivariate relationships in geosciences. Hydrology and Earth System Sciences, 20(8): 3183-3191. 10.5194/hess-20-3183-2016.
Hu, W., Si, B.C., Biswas, A., Chau, H.W., 2017. Temporally stable patterns but seasonal dependent controls of soil water content: Evidence from wavelet analyses. Hydrol. Process. 31 (21), 3697–3707. https://doi.org/10.1002/hyp.11289.
Huang, T., et al., 2020. How does precipitation recharge groundwater in loess aquifers? Evidence from multiple environmental tracers. J. Hydrol. 583 https://doi.org/10.1016/j.jhydrol.2019.124532.
Huang, Y., Chang, Q., Li, Z., 2018. Land use change impacts on the amount and quality of recharge water in the loess tablelands of China. Sci. Total Environ. 628–629, 443–452. https://doi.org/10.1016/j.scitotenv.2018.02.076.
Huang, Y., Evaristo, J., Li, Z., 2019. Multiple tracers reveal different groundwater recharge mechanisms in deep loess deposits. Geoderma 353, 204–212. https://doi.org/10.1016/j.geoderma.2019.06.041.
Huang, Y., Li, B., Li, Z., 2021. Conversion of degraded farmlands to orchards decreases groundwater recharge rates and nitrate gains in the thick loess deposits. Agric. Ecosyst. Environ. 314 https://doi.org/10.1016/j.agee.2021.107410.
Jackson, R.B., Berthrong, S.T., Cook, C.W., Jobbagy, E.G., McCulley, R.L., 2004. Comment on “A reservoir of nitrate beneath desert soils”. Science, 304(5667): 51; author reply 51. 10.1126/science.1094294.
Ji, W., et al., 2020. Legacy nitrate in the deep loess deposits after conversion of arable farmland to non-fertilized land uses for degraded land restoration. Land Degrad. Dev. 31 (11), 1355–1365. https://doi.org/10.1002/ldr.3532.
Ji, W., Huang, Y., Shi, P., Li, Z., 2021. Recharge mechanism of deep soil water and the response to land use change in the loess deposits. J. Hydrol. 592 https://doi.org/10.1016/j.jhydrol.2020.125817.
Jia, X., et al., 2018. Mineral N stock and nitrate accumulation in the 50 to 200m profile on the Loess Plateau. Sci. Total Environ. 633, 999–1006. https://doi.org/10.1016/j.scitotenv.2018.03.249.

Jia, X., Shao, M.A., Zhu, Y., Luo, Y., 2017a. Soil moisture decline due to afforestation across the Loess Plateau, China. Journal of Hydrology, 546: 113-122. 10.1016/j.jhydrol.2017.01.011.
Jia, X., Zhu, Y., Luo, Y., 2017b. Soil moisture decline due to afforestation across the Loess Plateau, China. J. Hydrol. 546, 113–122.
Jiao, W., et al., 2021. Observed increasing water constraint on vegetation growth over the last three decades. Nat. Commun. 12 (1), 3777. https://doi.org/10.1038/s41467-021-24016-9.
Jordanova, D., Jordanova, N., 2021. Updating the significance and paleoclimate implications of magnetic susceptibility of Holocene loessic soils. Geoderma 391. https://doi.org/10.1016/j.geoderma.2021.114982.
Ju, X.T., et al., 2009. Reducing environmental risk by improving N management in intensive Chinese agricultural systems. Proc. Natl. Acad. Sci. U. S. A. 106 (9), 3041–3046. https://doi.org/10.1073/pnas.0813417106.
Kaandorp, V.P., Broers, H.P., Velde, Y.v.d., Rozemeijer, J., Louw, P.G.B.d., 2021. Time lags of nitrate, chloride, and tritium in streams assessed by dynamic groundwater flow tracking in a lowland landscape. Hydrol. Earth Syst. Sci., 2525,: 3691–3711. 10.5194/hess-2525-3691-20212021.
Kuypers, M.M.M., Marchant, H.K., Kartal, B., 2018. The microbial nitrogen-cycling network. Nat. Rev. Microbiol. 16 (5), 263–276. https://doi.org/10.1038/nrmicro.2018.9.
Levy-Booth, D.J., Prescott, C.E., Grayston, S.J., 2014. Microbial functional genes involved in nitrogen fixation, nitrification and denitrification in forest ecosystems. Soil Biol. Biochem. 75, 11–25. https://doi.org/10.1016/j.soilbio.2014.03.021.
Li, J., Li, Z., Lü, Z., 2016. Analysis of spatiotemporal variations in land use on the Loess Plateau of China during 1986–2010. Environmental Earth Sciences 75 (11). https://doi.org/10.1007/s12665-016-5807-y.
Li, J., Peng, S., Li, Z., 2017. Detecting and attributing vegetation changes on China's Loess Plateau. Agric. For. Meteorol. 247, 260–270. https://doi.org/10.1016/j.agrformet.2017.08.005.
Li, Z., Si, B., 2018. Reconstructed Precipitation Tritium Leads to Overestimated Groundwater Recharge. Journal of Geophysical Research: Atmospheres 123 (17), 9858–9867. https://doi.org/10.1029/2018jd028405.
Li, H., Si, B., Li, M., 2018. Rooting depth controls potential groundwater recharge on hillslopes. J. Hydrol. 564, 164–174. https://doi.org/10.1016/j.jhydrol.2018.07.002.
Li, H., Si, B., Ma, X., Wu, P., 2019a. Deep soil water extraction by apple sequesters organic carbon via root biomass rather than altering soil organic carbon content. Sci. Total Environ. 670, 662–671. https://doi.org/10.1016/j.scitotenv.2019.03.267.
Li, H., Si, B., Wu, P., McDonnell, J.J., 2019b. Water mining from the deep critical zone by apple trees growing on loess. Hydrol. Process. 33 (2), 320–327. https://doi.org/10.1002/hyp.13346.
Li, B., Yang, Y., Li, Z., 2021. Combined effects of multiple factors on spatiotemporally varied soil moisture in China's Loess Plateau. Agric. Water Manag. 258 https://doi.org/10.1016/j.agwat.2021.107180.
Lin, R., Wei, K., 2006. Tritium profiles of pore water in the Chinese loess unsaturated zone: implications for estimation of groundwater recharge. J. Hydrol. 328 (1–2), 192–199.
Lindsay, E.A., Colloff, M.J., Gibb, N.L., Wakelin, S.A., 2010. The abundance of microbial functional genes in grassy woodlands is influenced more by soil nutrient enrichment than by recent weed invasion or livestock exclusion. Appl. Environ. Microbiol. 76 (16), 5547–5555. https://doi.org/10.1128/AEM.03054-09.
Liu, Z., Ma, P., Zhai, B., Zhou, J., 2019. Soil moisture decline and residual nitrate accumulation after converting cropland to apple orchard in a semiarid region: Evidence from the Loess Plateau. Catena 181. https://doi.org/10.1016/j.catena.2019.104080.
Liu, L., Zhang, K., Zhang, Z., 2016. An improved core sampling technique for soil magnetic susceptibility determination. Geoderma 277, 35–40. https://doi.org/10.1016/j.geoderma.2016.04.030.
Lu, X., et al., 2021. Nitrogen deposition accelerates soil carbon sequestration in tropical forests. Proc Natl Acad Sci U S A 118 (16). https://doi.org/10.1073/pnas.2020790118.
Lu, Y., Si, B., Li, H., Biswas, A., 2019. Elucidating controls of the variability of deep soil bulk density. Geoderma 348, 146–157. https://doi.org/10.1016/j.geoderma.2019.04.033.
Mihanović, H., Orlić, M., Pasarić, Z., 2009. Diurnal thermocline oscillations driven by tidal flow around an island in the Middle Adriatic. J. Mar. Syst. 78, S157–S168.
Niether, W., et al., 2017. Spatial-temporal soil moisture dynamics under different cocoa production systems. Catena 158, 340–349. https://doi.org/10.1016/j.catena.2017.07.011.
Padilla, F.M., Gallardo, M., Manzano-Agugliaro, F., 2018. Global trends in nitrate leaching research in the 1960–2017 period. Sci. Total Environ. 643, 400–413. https://doi.org/10.1016/j.scitotenv.2018.06.215.
Peng, S., Li, Z., 2018. Incorporation of potential natural vegetation into revegetation programmes for sustainable land management. Land Degrad. Dev. 29 (10), 3503–3511. https://doi.org/10.1002/ldr.3124.
Scanlon, B.R., Reedy, R.C., Bronson, K.F., 2008. Impacts of land use change on nitrogen cycling archived in semiarid unsaturated zone nitrate profiles, southern High Plains. Texas. Environ. Sci. Technol 42, 7566–7572. https://doi.org/10.1021/es800792w.
Sebilo, M., Mayer, B., Nicolardot, B., Pinay, G., Mariotti, A., 2013. Long-term fate of nitrate fertilizer in agricultural soils. Proc. Natl. Acad. Sci. U. S. A. 110 (45), 18185–18189. https://doi.org/10.1073/pnas.1305372110.
Shi, P., et al., 2021a. Impacts of deep-rooted fruit trees on recharge of deep soil water using stable and radioactive isotopes. Agric. For. Meteorol. 300 https://doi.org/10.1016/j.agrformet.2021.108325.
Shi, P., Huang, Y., Yang, C., Li, Z., 2021b. Quantitative estimation of groundwater recharge in the thick loess deposits using multiple environmental tracers and methods. J. Hydrol. https://doi.org/10.1016/j.jhydrol.2021.126895.
Si, B.C., 2008. Spatial Scaling Analyses of Soil Physical Properties: A Review of Spectral and Wavelet Methods. Vadose Zone J. 7 (2), 547. https://doi.org/10.2136/vzj2007.0040.
Si, B.C., Farrell, R.E., 2004. Scale-dependent relationship between wheat yield and topographic indices. Soil Sci. Soc. Am. J. 68 (2), 577–587.
Sigler, W.A., et al., 2020. Water and nitrate loss from dryland agricultural soils is controlled by management, soils, and weather. Agric. Ecosyst. Environ. 304 https://doi.org/10.1016/j.agee.2020.107158.
Tao, Z., Neil, E., Si, B., 2021. Determining deep root water uptake patterns with tree age in the Chinese loess area. Agric. Water Manag. 249 https://doi.org/10.1016/j.agwat.2021.106810.
Tashi, S., Singh, B., Keitel, C., Adams, M., 2016. Soil carbon and nitrogen stocks in forests along an altitudinal gradient in the eastern Himalayas and a meta-analysis of global data. Glob Chang Biol 22 (6), 2255–2268. https://doi.org/10.1111/gcb.13234.
Turkeltaub, T., Jia, X., Zhu, Y., Shao, M.A., Binley, A., 2018. Recharge and Nitrate Transport Through the Deep Vadose Zone of the Loess Plateau: A Regional-Scale Model Investigation. Water Resour. Res. 54 (7), 4332–4346. https://doi.org/10.1029/2017wr022190.
Vitousek, P.M., et al., 1997. Human Alteration of the Global Nitrogen Cycle: Sources and Consequences. Ecol. Appl. 7 (3), 737–750. https://doi.org/10.1890/1051-0761(1997)007[0737:haotgn]2.0.co;2.
Wang, Y., et al., 2020. Response of deep soil drought to precipitation, land use and topography across a semiarid watershed. Agric. For. Meteorol. 282–283 https://doi.org/10.1016/j.agrformet.2019.107866.
Wiens, J.A., 1989. Spatial scaling in ecology. Functional ecology 3 (4), 385–397.
Xia, W., et al., 2011. Autotrophic growth of nitrifying community in an agricultural soil. ISME J. 5 (7), 1226–1236. https://doi.org/10.1038/ismej.2011.5.
Yang, S.-H., et al., 2020. Variation of deep nitrate in a typical red soil Critical Zone: Effects of land use and slope position. Agric. Ecosyst. Environ. 297 https://doi.org/10.1016/j.agee.2020.106966.
Yang, W., Jin, F., Si, Y., Li, Z., 2021. Runoff change controlled by combined effects of multiple environmental factors in a headwater catchment with cold and arid climate in northwest China. Sci. Total Environ. 756, 143995 https://doi.org/10.1016/j.scitotenv.2020.143995.
Ye, L., Fang, L., Shi, Z., Deng, L., Tan, W., 2019. Spatio-temporal dynamics of soil moisture driven by 'Grain for Green' program on the Loess Plateau, China. Agric. Ecosyst. Environ. 269, 204–214. https://doi.org/10.1016/j.agee.2018.10.006.
Yu, C., et al., 2019. Managing nitrogen to restore water quality in China. Nature 567 (7749), 516–520. https://doi.org/10.1038/s41586-019-1001-1.
Yuan, H., et al., 2020. Co-application of a biochar and an electric potential accelerates soil nitrate removal while decreasing N2O emission. Soil Biol. Biochem. 149 https://doi.org/10.1016/j.soilbio.2020.107946.
Zhang, Z., Li, M., Si, B., Feng, H., 2018. Deep rooted apple trees decrease groundwater recharge in the highland region of the Loess Plateau, China. Sci. Total Environ. 622–623, 584–593. https://doi.org/10.1016/j.scitotenv.2017.11.230.
Zhao, Y., et al., 2011. Factors controlling the spatial patterns of soil moisture in a grazed semi-arid steppe investigated by multivariate geostatistics. Ecohydrology 4 (1), 36–48. https://doi.org/10.1002/eco.121.
Zheng, W., Wang, S., Tan, K., Lei, Y., 2020. Nitrate accumulation and leaching potential is controlled by land-use and extreme precipitation in a headwater catchment in the North China Plain. Sci. Total Environ. 707, 136168 https://doi.org/10.1016/j.scitotenv.2019.136168.
Zhu, H., et al., 2018. Soil organic carbon prediction based on scale-specific relationships with environmental factors by discrete wavelet transform. Geoderma 330, 9–18.
Zhu, Y., Shao, M., 2008. Variability and pattern of surface moisture on a small-scale hillslope in Liudaogou catchment on the northern Loess Plateau of China. Geoderma 147 (3–4), 185–191. https://doi.org/10.1016/j.geoderma.2008.08.012.